Delamination of non-linear viscoelastic beams under bending in the plane of layers

Victor I. Rizov*

*Department of Technical Mechanics, University of Architecture, Civil Engineering and Geodesy,
1 Chr. Smirnensky Blvd., 1046-Sofia, Bulgaria*

Abstract. This paper deals with delamination analysis of non-linear viscoelastic multilayered beam subjected to bending in the plane of the layers. For this purpose, first, a non-linear viscoelastic model is presented. In order to take into account the non-linear viscoelastic behaviour, a non-linear spring and a non-linear dashpot are assembled in series with a linear spring connected in parallel to a linear dashpot. The behaviours of the non-linear spring and dashpot are described by applying non-linear stress-strain and stress-rate of strain relationships, respectively. The constitutive law of the model is derived. Due to the non-linear spring and dashpot, the constitutive law is non-linear. This law is used for describing the time-dependent mechanical behaviour of the beam under consideration. The material properties involved in the constitutive law vary along the beam length due to the continuous material inhomogeneity of the layers. Solution of the strain energy release rate for the delamination is obtained by analyzing the balance of the energy with considering of the non-linear viscoelastic behaviour. The strain energy release rate is found also by using the complementary strain energy for verification. A parametric study is carried-out by using the solution obtained. The solutions derived and the results obtained help to understand the time-dependent delamination of non-linear viscoelastic beams under loading in the plane of layers.

Keywords: delamination; inhomogeneous material; multilayered beam; non-linear viscoelastic behaviour; stress-strain-time relationship

1. Introduction

The search for efficacious structural solutions in various areas of modern engineering leads very often to applications of highly sophisticated continuously inhomogeneous materials whose properties are continuous functions of coordinates. One kind of these materials known as functionally graded materials has attracted considerable attention in academic circles around the globe in the recent decades (Butcher *et al.* 1999, Faleh *et al.* 2018, Gasik, 2010, Han *et al.* 2001, Hedia *et al.* 2014, Hirai and Chen, 1999, Khaled Amara *et al.* 2016, Mahamood and Akinlabi, 2017). Functionally graded materials are relatively new (they have been introduced in 1980's) inhomogeneous composites produced by continuously mixing of two or more constituent materials. The continuous variation of the microstructure of these novel materials along one or

---

more directions in the solid can be tailored during production process so as to obtain the desired distribution of the material properties within the structural member (Bouazza and Zenkour, 2020, Civalek *et al.* 2021, Dastjerdi *et al.* 2020, Derbale *et al.* 2021, El-Galy *et al.* 2019, Saiyathibrahim *et al.* 2016, Shrikantha and Gangadharan, 2014, Wu *et al.* 2014). Therefore, nowadays, these advanced engineering materials play an important role and their applicability increases continuously (Akbaş *et al.* 2021, Ellali *et al.* 2021, Markworth *et al.* 1995, Miyamoto *et al.* 1999, Nemat-Allal *et al.* 2011, Raad *et al.* 2019, Ridha *et al.*2019, Toudehdehghan *et al.* 2017).

The multilayered inhomogeneous structures are built-up by adhesively bonded layers with different thicknesses and material properties. There are many advantageous properties of multilayered materials over the conventional homogeneous structural materials. Among them, the high strength-to-weight and stiffness-to-weight ratios are of special importance. That is why, these materials are particularly suitable for building of light-weight structures. The multilayered structural materials have found also application in aggressive environment. Besides, various structural components like beams, columns and plates of concrete or steel strengthened by adhesively bonded layers of polymer composites to some extent can also be considered as multilayered structures. Reinforced-concrete beams strengthened by laminated composites are analyzed with considering the influence of temperature and the number of cross-play layers (Mokhtar Bouazza *et al.* 2019). Higher-order shear theories are applied for studying the non-linear response of composite beams to a temperature variation and moisture concentrations (Mokhtar Bouazza *et al.* 2014). Thermal buckling behaviour of laminated composite beams is investigated by using hyperbolic refined shear deformation theory (Mokhtar Bouazza *et al.* 2019). An analytical approach for analyzing the buckling of cross-play and angle-play composite beams under hygro-thermal-mechanical loading is presented in (Mokhtar Bouazza and Ashraf M. Zenkour, 2020). The wave propagation in a functionally graded plate is studied by micromechanical approaches (Mokhtar Ellali *et al.* 2022). First order shear deformation theory is applied for studying the thermal buckling of a functionally graded rectangular plate (Atmane *et al.* 2016). An analytical modelling of the thermal buckling behaviour of functionally graded rectangular plates is carried-out (Mokhtar Bouazza *et al.* 2015). Bending behaviour of laminated composite plates is investigated using a model based on multilayer plate theory (Mokhtar Bouazza *et al.* 2019). The influence of varying material properties and volume fraction of the constituent materials on bending behaviour of a functionally graded plate is examined theory (Mokhtar Bouazza *et al.* 2018). An exact analytical solution for buckling behaviour of magnetoelectroelastic plate resting on Pasternak foundation is derived in (Mokhtar Ellali *et al.* 2018). An exact analytical solution for buckling analysis of symmetrically cross-play laminated plates is developed in (Tawfiq Becheri *et al.* 2016). The separation of layers or delamination is the basic disadvantage of multilayered material and structures (Dolgov 2005, Dolgov 2016). Delamination reduces the strength, stiffness and load-bearing capacity of multilayered structures and affects their proper working. Therefore, the durability and reliability of these structures depends in high degree on their delamination behaviour.

In their life-time, the multilayered structures very often exhibit non-linear viscoelastic behaviour. Therefore, from practical view point, it is interesting to evaluate the influence of non-linear viscoelastic mechanical behaviour on the delamination in these structures. It should also be mentioned that there are situations in which the multilayered beam structures are loaded in bending in the plane of layers. For these reasons, the purpose of the paper is to develop a delamination analysis that take into account the non-linear viscoelastic behaviour of multilayered inhomogeneous beams subjected to bending in the plane of layers. Here, a model consisting of
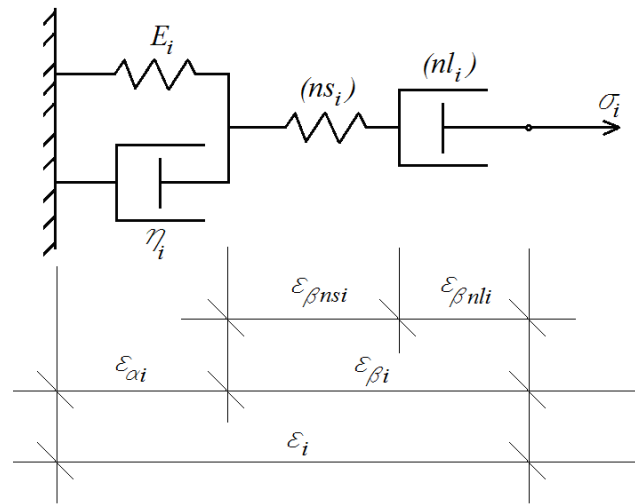
Fig. 1 Non-linear viscoelastic model

linear as well as non-linear springs and dashpots is introduced. The constitutive law of the model is obtained by considering the strains in the components of the model under stress that varies non-linearly with time. The model is used to describe the non-linear viscoelastic behaviour of the multilayered beam when deriving solution of the strain energy release rate. It should be noted here that there are other studies on the in-plane bending mechanical behaviour of laminated beams from the perspective of the delamination mechanism (one of the pioneer studies in this area are (Donaldson 1988, Donaldson and Mall 1989)). These studies, however, do not deal with beams exhibiting non-linear viscoelastic behaviour. Besides, these studies (Donaldson 1988, Donaldson and Mall 1989) treat the laminated beams as homogeneous bodies (without layers). Therefore, the novelty of the present paper consists in two facts. First, a non-linear viscoelastic model is used when analyzing the delamination and, second, the beam configuration subjected to bending in the plane of layers studied in the present paper is multilayered in contrast to some previous studies which deal with delamination in structures loaded transversally to the layers (Rizov 2020a, b, 2021, 2022, Rizov and Altenbach 2019, 2022). A parametric study is performed by the solution of the strain energy release rate derived in the present paper.

2. Analysis of the strain energy release rate with considering of non-linear viscoelastic behaviour

Since the multilayered beam under consideration in the present paper has non-linear viscoeastic behaviour, the well-known linear theory of viscoelasticity must be replaced by a non-linear theory (the latter uses non-linear viscoelastic models). Here, in order to take into account the viscoelastic behaviour of the multilayered beam a simple non-linear Maxwell model consisting of a non-linear spring, ns_i, and a non-linear dashpot, nl_i, is connected in series to the classical Kelvin model representing a combination of a linear dashpot with coefficient of viscosity, η_i, connected in parallel to a linear spring with modulus of elasticity, E_i as shown in Fig. 1. The model in Fig. 1 is under stress, σ_i, that changes with time, t, according to the following parabolic law

$$\sigma_i = v_{\sigma i} t^2, \tag{1}$$

where $v_{\sigma i}$ is a parameter which controls the change of the stress.

The strain in the model is written as

$$\varepsilon_i = \varepsilon_{\alpha i} + \varepsilon_{\beta i}, \tag{2}$$

where $\varepsilon_{\alpha i}$ is the linear strain in the linear spring and the linear dashpot (Fig. 1). The non-linear strain, $\varepsilon_{\beta i}$, is presented as a sum of strain, $\varepsilon_{\beta nsi}$, in the non-linear spring and strain, $\varepsilon_{\beta nli}$, in the non-linear dashpot

$$\varepsilon_{\beta i} = \varepsilon_{\beta nsi} + \varepsilon_{\beta nli}. \tag{3}$$

First, the linear strain is derived. For this purpose, the stresses in the linear spring and linear dashpot, σ_{Ei} and $\sigma_{\eta i}$, are expressed as

$$\sigma_{Ei} = \varepsilon_{\alpha i} E_i, \tag{4}$$

$$\sigma_{\eta i} = \dot{\varepsilon}_{\alpha i} \eta_i, \tag{5}$$

where $\dot{\varepsilon}_{\alpha i}$ is the first derivative of the $\varepsilon_{\alpha i}$ with respect to time. The equation of equilibrium of the linear spring and linear dashpot is written as

$$\sigma_{Ei} + \sigma_{\eta i} = \sigma_i. \tag{6}$$

By combining of (1), (4), (5) and (6), one obtains

$$\dot{\varepsilon}_{\alpha i} + \mu_i \varepsilon_{\alpha i} = \rho_i t^2, \tag{7}$$

where

$$\mu_i = \frac{E_i}{\eta_i}, \tag{8}$$

$$\rho_i = \frac{v_{\sigma i}}{\eta_i}. \tag{9}$$

The solution of differential Eq. (7) is written as

$$\varepsilon_{\alpha i} = C_1 e^{-\mu_i t} + \overline{\varepsilon_{\alpha i}}, \tag{10}$$

where C_1 is the integration constant, $\overline{\varepsilon_{\alpha i}}$ is a particular solution. The initial condition and the particular solution are expressed as

$$\varepsilon_{\alpha i}(0) = 0 \tag{11}$$

and

$$\overline{\varepsilon_{\alpha i}} = D t^2 + H t + L, \tag{12}$$

where D, H and L are constants. After performing some mathematical manipulations, one derives

$$\varepsilon_{\alpha i}(t) = \frac{2\rho_i}{\mu_i^3} \left(1 - e^{-\mu_i t} \right) + \frac{\rho_i}{\mu_i} t^2 - \frac{2\rho_i}{\mu_i^2} t. \tag{13}$$

The stress, σ_{nsi}, in the non-linear spring is related to the strain, $\varepsilon_{\beta nsi}$, through the following non-linear relationship (Lukash 1978)

$$\sigma_{nsi} = \frac{\varepsilon_{\beta nsi}}{q_i + r_i \varepsilon_{\beta nsi}}, \tag{14}$$
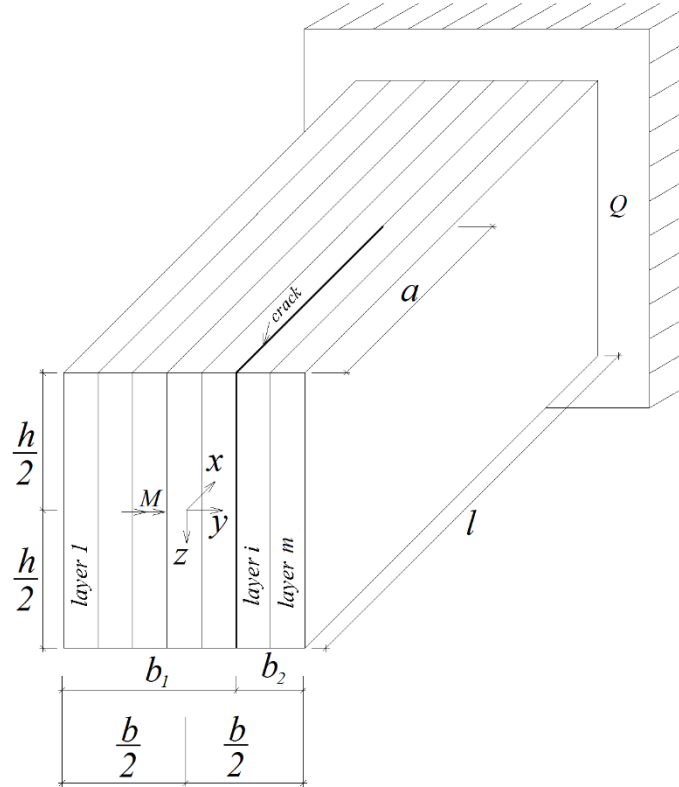
Fig. 2 Multilayered beam subjected to bending in the plane of layers

where q_i and r_i are material properties. Fig. 1 indicates that

$$\sigma_{nsi} = \sigma_i. \tag{15}$$

By combining of (1), (14) and (15), one obtains

$$\varepsilon_{\beta nsi}(t) = \frac{v_{\sigma i} t^2 q_i}{1 - v_{\sigma i} t^2 r_i}. \tag{16}$$

The following non-linear relationship between the stress, σ_{nli}, and the first derivative of strain with respect to time, $\dot{\varepsilon}_{\beta nli}$, in the non-linear dashpot is used (Lukash 1978)

$$\sigma_{nli} = \frac{\dot{\varepsilon}_{\beta nli}}{p_i + f_i \dot{\varepsilon}_{\beta nli}}, \tag{17}$$

where p_i and f_i are material properties.

It follows from Fig. 1 that

$$\sigma_{nli} = \sigma_i. \tag{18}$$

From (17) and (18), one obtains

$$\dot{\varepsilon}_{\beta nli} = \frac{\sigma_i p_i}{1 - \sigma_i f_i}. \tag{19}$$

By using of (1), and (19) and performing some mathematical transformations, one derives

$$\varepsilon_{\beta n l i}(t) = -\frac{p_i t}{f_i} + \frac{p_i}{2 f_i \sqrt{v_{\sigma i} f_i}} \ln\left|\frac{\sqrt{v_{\sigma i} f_i} + v_{\sigma i} f_i t}{\sqrt{v_{\sigma i} f_i} - v_{\sigma i} f_i t}\right|. \tag{20}$$

Finally, by combining of (1), (2), (3), (9), (13), (16) and (20), one obtains

$$\varepsilon_i(t) = \frac{2\sigma_i}{\eta_1 \mu_i^3 t^2}\left(1 - e^{-\mu_i t}\right) + \frac{\sigma_i}{\eta_i \mu_i} - \frac{2\sigma_i}{\eta_i \mu_i^2 t} + \frac{\sigma_i q_i}{1 - \sigma_i r_i} - \frac{p_i t}{f_i} + \frac{p_i t}{2 f_i \sqrt{\sigma_i f_i}} \ln\left|\frac{1 + \sqrt{\sigma_i f_i}}{1 - \sqrt{\sigma_i f_i}}\right|. \tag{21}$$

Formula (21) expresses the constitutive law of the non-linear viscoelastic model displayed in Fig. 1. Due to the non-linear spring and the non-linear dashpot included in the model, the stress-strain-time constitutive law (21) is non-linear. This constitutive law is used for describing of non-linear viscoelastic time-dependent mechanical behaviour of the delaminated multilayered inhomogeneous cantilever beam member displayed in Fig. 2.

The beam has an arbitrary number of longitudinal layers of different widths and material properties. The width, height and length of the beam are denoted by b, h and l, respectively (Fig. 2). The beam is clamped in section, Q. A delamination crack is located between layers so as the widths of the left-hand and right-hand crack arms are b_1 and b_2, respectively. The length of the delamnation crack is denoted by a. The layers exhibit continuous material inhomogeneity along the length of the beam. Therefore, the material properties which are involved in the constitutive law (21) vary continuously in longitudinal direction of the beam. The following exponential laws are used for describing of the distribution of material properties in the i-th layer along the beam length

$$E_i = E_{0i} e^{g_{Ei}\frac{x}{l}}, \tag{22}$$

$$\eta_i = \eta_{0i} e^{g_{\eta i}\frac{x}{l}}, \tag{23}$$

$$q_i = q_{0i} e^{g_{qi}\frac{x}{l}}, \tag{24}$$

$$r_i = r_{0i} e^{g_{ri}\frac{x}{l}}, \tag{25}$$

$$p_i = p_{0i} e^{g_{pi}\frac{x}{l}}, \tag{26}$$

$$f_i = f_{0i} e^{g_{fi}\frac{x}{l}}, \tag{27}$$

where

$$i = 1,2,\ldots,m, \tag{28}$$

$$0 \le x \le l. \tag{29}$$

In formulae (22)-(29), x is the longitudinal centroidal axis of the beam, m is the number of layers, E_{0i}, η_{0i}, q_{0i}, r_{0i}, p_{0i} and f_{0i} are the values of E_i, η_i, q_i, r_i, p_i and f_i at free end of the beam, respectively. The parameters, g_{Ei}, $g_{\eta i}$, g_{qi}, g_{ri}, g_{pi} and g_{fi}, control the variation of E_{0i}, η_{0i}, q_{0i}, r_{0i}, p_{0i} and f_{0i} in the i-th layer in longitudinal direction of the beam, respectively.

The beam is under conditions of bending in the plane of the layers. A bending moment, M, is applied at the free end of the left-hand crack arm as shown in Fig. 2. Therefore, the right-hand crack arm is free of stresses. The variation of the bending moment with time is described as

$$M = vt^2, \tag{30}$$
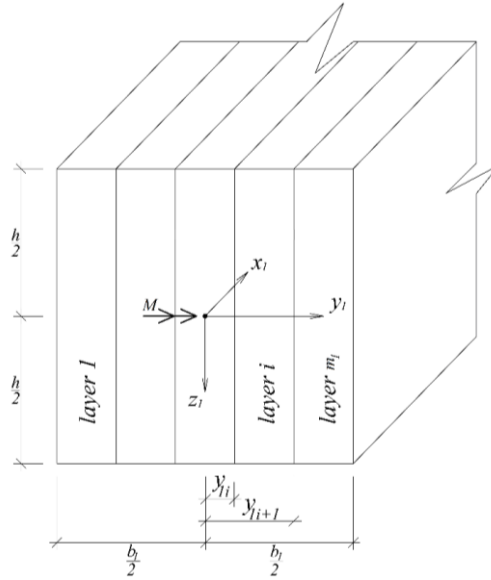
Fig. 3 Cross-section of the left-hand crack arm

where v is a parameter that controls the loading.

A solution of the strain energy release rate for the delamination crack in Fig. 2 that takes into account the non-linear viscoelastic behaviour is derived by analyzing the balance of the energy in the beam structure. The balance is written as

$$M\delta\varphi = \frac{\partial U}{\partial a}\delta a + Gh\delta a\,,\tag{31}$$

where ϕ is the angle of rotation of the free end of the left-hand crack arm, U is the strain energy in the beam, G is the strain energy release rate, δa is a small increase of the crack length. From (31), one obtains

$$G = \frac{1}{h}\left(M\frac{\partial\varphi}{\partial a} - \frac{\partial U}{\partial a} \right).\tag{32}$$

The angle, ϕ, is found by applying the integrals of Maxwell-Mohr. The result is

$$\varphi = \int_{0}^{a} \kappa_1 dx + \int_{a}^{l} \kappa_2 dx\,,\tag{33}$$

where κ_1 and κ_2 are the curvatures of the left-hand crack arm and the un-cracked beam portion, $a \leq x \leq l$, respectively.

The following approach is used in order to determine κ_1. First, the equation of equilibrium of the elementary forces in the cross-section of the left-hand is written as

$$M = \sum_{i=1}^{i=m_l} \left(y_{1i+1} - y_{1i}\right)\int_{-\frac{h}{2}}^{\frac{h}{2}} \sigma_i z_1 dz_1\,,\tag{34}$$

where m_1 is the number of layers in the left-hand crack arm, y_{1i} and y_{1i+1} are the coordinates of the left-hand and right-hand lateral surfaces of the i-th layer, σ_i is the stress in the layer, z_1 is the vertical axis (Fig. 3), M is found by (30). The constitutive law (21) expresses the strain as a non-linear function of stress. Therefore, σ_i that is involved in (34) can not be determined explicitly from (21). This problem is solved here by expressing z_1 and dz_1 as functions of σ_i. The boundaries of integration in (34) are changed as

$$M = \sum_{i=1}^{i=m_1} \left(y_{1i+1} - y_{1i} \right) \int_{\sigma_{\psi i}}^{\sigma_{\theta i}} \sigma_i z_1 dz_1, \tag{35}$$

where $\sigma_{\psi i}$ and $\sigma_{\theta i}$ are the stresses in the upper and lower surface of the i-th layer.

The distribution of the strains is expressed by applying the Bernoulli's hypothesis for plane sections since beams of high length to height ratio are under consideration in this paper. Thus, the distribution of strains, ε, in the left-crack arm is written as

$$\varepsilon = \kappa_1 z_1. \tag{36}$$

From (36), one derives

$$z_1 = \frac{\varepsilon}{\kappa_1}. \tag{37}$$

The quantities, z_1 and dz_1, which are involved in (35) are expressed in the following manner. First, by using of (21) and (37), one obtains

$$z_1 = \frac{1}{\kappa_1} \left[\frac{2\sigma_i}{\eta_1 \mu_i^3 t^2} \left(1 - e^{-\mu_i t} \right) + \frac{\sigma_i}{\eta_i \mu_i} \frac{2\sigma_i}{\eta_i \mu_i^2 t} + \frac{\sigma_i q_i}{1 - \sigma_i r_i} - \frac{p_i t}{f_i} + \frac{p_i t}{2 f_i \sqrt{\sigma_i f_i}} \ln \left| \frac{1 + \sqrt{\sigma_i f_i}}{1 - \sqrt{\sigma_i f_i}} \right| \right]. \tag{38}$$

From (38), the quantity, dz_1, is found as

$$dz_1 = \frac{1}{\kappa_1} \left\{ \frac{2}{\eta_1 \mu_i^3 t^2} \left(1 - e^{-\mu_i t} \right) + \frac{1}{\eta_i \mu_i} \frac{2}{\eta_i \mu_i^2 t} + \frac{q_i}{\left(1 - \sigma_i r_i \right)^2} + \right.$$
$$\left. + \frac{p_i t}{2 f_i^{\frac{3}{2}}} \left[-\frac{1}{2\sigma_i^{\frac{3}{2}}} \ln \left| \frac{1 + \sqrt{\sigma_i f_i}}{1 - \sqrt{\sigma_i f_i}} \right| + \frac{\sqrt{f_i}}{\sigma_i \left(1 - f_i \sigma_i \right)} \right] \right\} d\sigma_i. \tag{39}$$

In order to determine the stresses, $\sigma_{\psi i}$ and $\sigma_{\theta i}$, the following equations are written by using (21) and (36)

$$\kappa_1 \left(-\frac{h}{2} \right) = \frac{2\sigma_{\psi i}}{\eta_1 \mu_i^3 t^2} \left(1 - e^{-\mu_i t} \right) + \frac{\sigma_{\psi i}}{\eta_i \mu_i} \frac{2\sigma_{\psi i}}{\eta_i \mu_i^2 t} + \frac{\sigma_{\psi i} q_i}{1 - \sigma_i r_i} - \frac{p_i t}{f_i} + \frac{p_i t}{2 f_i \sqrt{\sigma_{\psi i} f_i}} \ln \left| \frac{1 + \sqrt{\sigma_{\psi i} f_i}}{1 - \sqrt{\sigma_{\psi i} f_i}} \right|, \tag{40}$$

$$\kappa_1 \frac{h}{2} = \frac{2\sigma_{\theta i}}{\eta_1 \mu_i^3 t^2} \left(1 - e^{-\mu_i t} \right) + \frac{\sigma_{\theta i}}{\eta_i \mu_i} \frac{2\sigma_{\theta i}}{\eta_i \mu_i^2 t} + \frac{\sigma_{\theta i} q_i}{1 - \sigma_{\theta i} r_i} - \frac{p_i t}{f_i} + \frac{p_i t}{2 f_i \sqrt{\sigma_{\theta i} f_i}} \ln \left| \frac{1 + \sqrt{\sigma_{\theta i} f_i}}{1 - \sqrt{\sigma_{\theta i} f_i}} \right|, \tag{41}$$

where $i = 1, 2, \ldots, m_1$. Equations (35), (40) and (41) are solved with respect to $\sigma_{\psi i}$, $\sigma_{\theta i}$ and κ_1 by using the MatLab computer program at various values of time.

Analogous approach is used to determine the curvature of the beam in the un-cracked portion and the stresses at the upper and lower surfaces of the layers, $\sigma_{u\psi i}$ and $\sigma_{u\theta i}$, respectively. For this

purpose, m_1, z_1, $\sigma_{\psi i}$, $\sigma_{\theta i}$ and κ_1 are replaced with $m_\rightleftarrows$, z_2, $\sigma_{u\psi i}$, $\sigma_{u\theta i}$ and κ_2 in Eqs. (35), (40) and (41) where z_2 is the vertical axis of the cross-section of the beam in the un-cracked portion. Then the MatLab is used to solve Eqs. (35), (40) and (41) with respect to $\sigma_{u\psi i}$, $\sigma_{u\theta i}$ and κ_2 at various values of time.

The strain energy that is involved in (32) is found as

$$U = U_1 + U_2, \tag{42}$$

where U_1 and U_2 are the strain energies in the left-hand crack arm and the un-cracked beam portion, respectively. The quantity, U_1, is written as

$$U_1 = \sum_{i=1}^{i=m_1} \left(y_{1i+1} - y_{1i} \right) \int_0^a \int_{\sigma_{\psi i}}^{\sigma_{\theta i}} u_{0i} dx dz_1, \tag{43}$$

where u_{0i} is the strain energy density in the i-th layer, dz_1 is obtained by (39), $\sigma_{\psi i}$ and $\sigma_{\theta i}$ are determined from Eqs. (35), (40) and (41).

In principle, the strain energy density can be found as

$$u_{0i} = \int_0^{\sigma_i} \sigma_i d\varepsilon. \tag{44}$$

However, in the case under consideration σ_i can not be determined explicitly from (21) since (21) represents a non-linear function of σ_i. Therefore, u_{0i} is written as

$$u_{0i} = \sigma_i \varepsilon_i - \int_0^{\varepsilon_i} \varepsilon_i d\sigma_i. \tag{45}$$

The strain energy cumulated in the un-cracked beam portion is found by applying (43). For this purpose, m_1, z_1, $\sigma_{\psi i}$, $\sigma_{\theta i}$ and u_{0i} are replaced with $m_\rightleftarrows$, z_2, $\sigma_{u\psi i}$, $\sigma_{u\theta i}$ and u_{0ui}, respectively (u_{0ui} is the strain energy density in the i-th layer of the un-cracked beam portion). Besides, the lower and the upper boundaries of integration along $x_\rightleftarrows$ are written as $a_\rightleftarrows$ and l, respectively.

By combining of (32), (33), (42) and (43), one derives

$$G = \frac{1}{h} \left[M\left(\kappa_1 - \kappa_2 \right) - \left(y_{1i+1} - y_{1i} \right) \sum_{i=1}^{i=m_1} \int_{\sigma_{\psi i}}^{\sigma_{\theta i}} u_{0i} dz_1 + \left(y_{2i+1} - y_{2i} \right) \sum_{i=1}^{i=m} \int_{\sigma_{u\psi i}}^{\sigma_{u\theta i}} u_{0ui} dz_2 \right) \right], \tag{46}$$

where y_{2i} and y_{2i+1} are the coordinates of the left-hand and right-hand lateral surfaces of the i-th layer in the un-cracked beam portion. The curvatures, the stresses and the strain energy densities involved in (46) are determined at $x = a$. The MatLab computer program is used to perform the integration in (46). Expression (46) is applied to obtain the strain energy release rate at various values of time.

The strain energy release rate is obtained also by using the complementary strain energy, U^*, in the beam member for verification. For this purpose, the strain energy release rate is written as

$$G = \frac{dU^*}{dA}. \tag{47}$$

The increase of the crack area, dA, is found as

$$dA = hda, \tag{48}$$

Victor I. Rizov
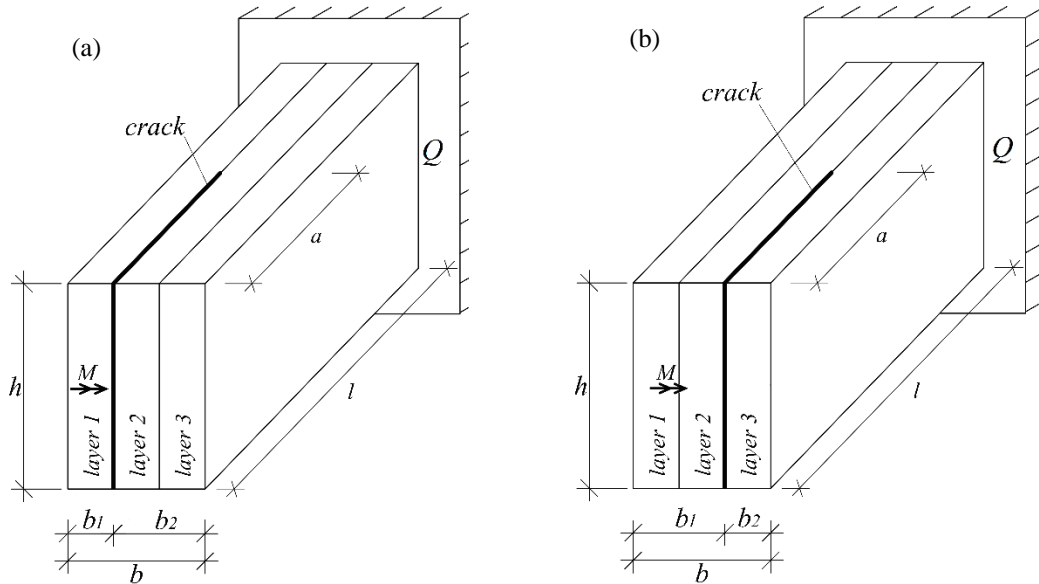
Fig. 4 Three-layered beam structure (a) with delamination between layers 1 and 2, (b) with delamination between layers 2 and 3

where da is an elementary increase of the crack length. By using (47) and (48), one derives

$$G = \frac{dU^*}{hda}. \tag{49}$$

The complementary strain energy is obtained as

$$U^* = U_1^* + U_2^*, \tag{50}$$

where U_1^* and U_2^* are the complementary strain energies cumulated in the left-hand crack arm and in the un-cracked beam portion, respectively.

The quantity, U_1^*, is written as

$$U_1^* = \sum_{i=1}^{i=m_1} \left(y_{1i+1} - y_{1i} \right) \int_0^a \int_{\sigma_{yi}}^{\sigma_{\theta i}} u_{0i}^* dx dz_1, \tag{51}$$

where the complementary strain energy density, u_{0i}^*, in the i-th layer is derived as

$$u_{0i}^* = \int_0^{\varepsilon_i} \varepsilon_i d\sigma_i. \tag{52}$$

The complementary strain energy in the un-cracked beam portion is found as

$$U_2^* = \sum_{i=1}^{i=m} \left(y_{2i+1} - y_{2i} \right) \int_a^l \int_{\sigma_{uyi}}^{\sigma_{u\theta i}} u_{0ui}^* dx dz_2, \tag{53}$$

where u_{0ui}^* is the complementary strain energy density.
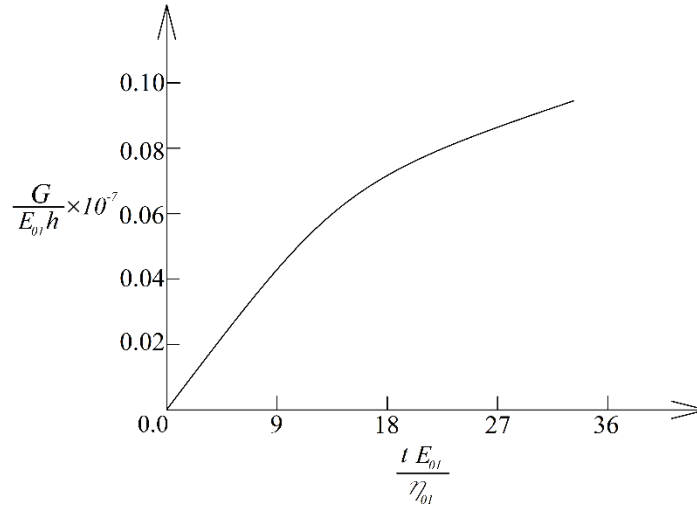
Fig. 5 Variation of the non-dimensional strain energy release rate with non-dimensional time

By combining of (49), (50), (51) and (53), one obtains

$$G = \frac{1}{h} \left[\sum_{i=1}^{i=m_1} \left(y_{1i+1} - y_{1i} \right) \int_{\sigma_{yi}}^{\sigma_{0i}} u_{0i}^* dz_1 - \sum_{i=1}^{i=m} \left(y_{2i+1} - y_{2i} \right) \int_{\sigma_{uyi}}^{\sigma_{u0i}} u_{0ui}^* dz_2 \right], \tag{54}$$

where the stresses and complementary strain energy densities are found at $x = a$. Formula (54) is used to determine the strain energy release rate at various values of time.

The integration in (54) is carried-out by using the MatLab computer program. The strain energy release rates obtained by (54) are exact matches of these found by (46) which proves the correctness of the analysis.

3. Parametric investigation

Parametric investigations are performed in this section of the paper. For this purpose, calculations of the strain energy release rate are carried-out by applying (46).

It is assumed that $b = 0.010$ m, $h = 0.015$ m and $v = 0.6 \times 10^{-7}$ Nm/s². Two beam members with three layers are considered in the parametric investigation in order to evaluate the effect of delamination crack location along the width of the beam on the strain energy release rate (Fig. 4). A delamination crack is located between layers 1 and 2 (Fig. 4(a)) and between layers 2 and 3 (Fig. 4(b)). The beams are clamped in section Q (Fig. 4).

First, the variation of the strain energy release rate with time induced by the non-linear viscoelastic behaviour of the beam and by the change of the external bending moment with time is investigated. The strain energy release rate is expressed in non-dimensional form by using the formula $G_N = G/(E_{01}h)$. Fig. 5 displays the variation of the strain energy release rate with non-dimensional time for the beam with crack located between layers 1 and 2 (the time is expressed in non-dimensional form by using the formula $t_N = tE_{01}/\eta_{01}$). It can be found from Fig. 5 that the strain energy release rate increases with time.

Victor I. Rizov
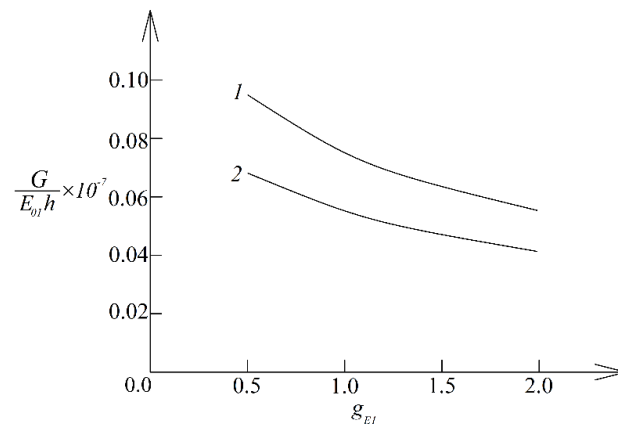
Fig. 6 Variation of the non-dimensional strain energy release rate with g_{E1} (curve 1 - for beam with delamination between layers 1 and 2, curve 2 - for beam with delamination between layers 2 and 3)
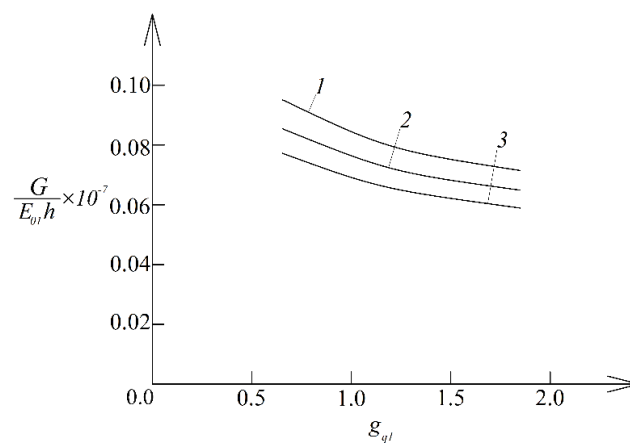
Fig. 7 Variation of the non-dimensional strain energy release rate with g_{q1} (curve 1 - at $a/l = 0.4$, curve 2 - at $a/l = 0.6$, curve 3 - at $a/l = 0.8$)
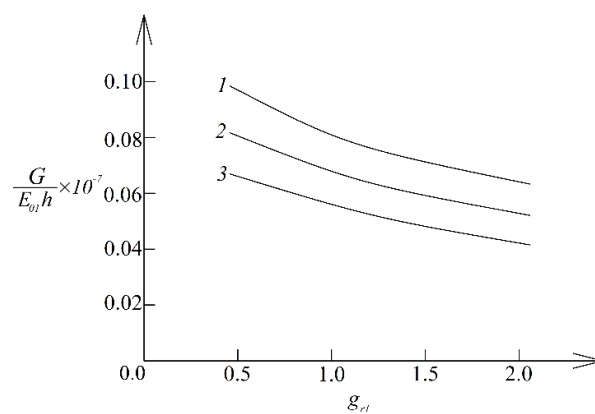
Fig. 8 Variation of the non-dimensional strain energy release rate with g_{r1} (curve 1 - at $g_{p1} = 0.5$, curve 2 - at $g_{p1} = 0.7$, curve 3 - at $g_{p1} = 0.9$)
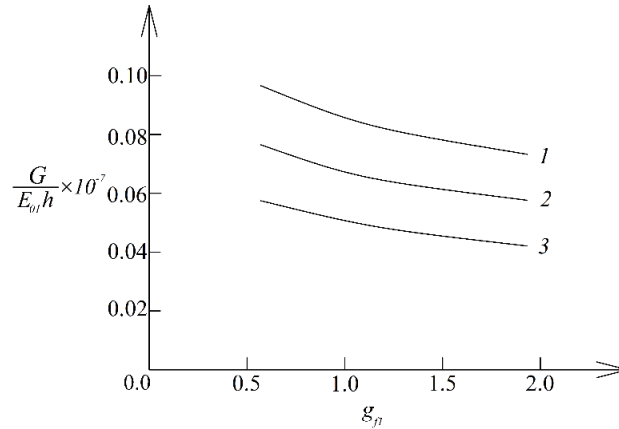
Fig. 9 Variation of the non-dimensional strain energy release rate with g_{f1} (curve 1 - at $g_{E2}/g_{E1} = 0.5$, curve 2 - at $g_{E2}/g_{E1} = 1.5$, curve 3 - at $g_{E2}/g_{E1} = 2.5$)
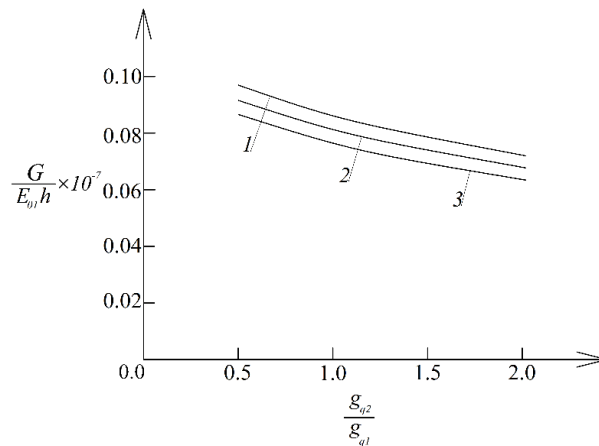
Fig. 10 Variation of the non-dimensional strain energy release rate with g_{q2}/g_{q1} ratio (curve 1 - at $g_{r2}/g_{r1} = 0.5$, curve 2 - at $g_{r2}/g_{r1} = 1.5$, curve 3 - at $g_{r2}/g_{r1} = 2.5$)

The variation of the strain energy release rate with g_{E1} for the beam with crack located between layers 1 and 2, and for the beam with crack between layers 2 and 3 is displayed in Fig. 6. The curves in Fig. 6 indicate that the strain energy release rate is higher when the delamination is between layers 1 and 2 (this due to fact that in this case the stiffness of left-hand crack arm is lower). Fig. 6 shows also that the strain energy release rate decreases with increasing of g_{E1}.

The influence of the change of q_1 in layer 1 along the length of the beam is analyzed too (this change is characterized by g_{q1}). Fig. 7 shows the variation of the strain energy release rate with g_{q1} for three a/l ratios. It can be observed in Fig. 7 that the strain energy release rate decreases with increasing of g_{q1}. The increase of a/l ratio leads also to decrease of the strain energy release rate (Fig. 7).

The effect of g_{r1} and g_{p1} on the strain energy release rate is illustrated in Fig. 8. It can be found from Fig. 8 that the strain energy release rate decreases with increasing of g_{r1} and g_{p1}.

Fig. 9 shows the variation of the strain energy release rate with g_{f1} at three g_{E2}/g_{E1} ratios. One can observe in Fig. 9 that the strain energy release rate decreases with increasing of g_{f1}. Increase of g_{E2}/g_{E1} ratio also induces decrease of the strain energy release rate (Fig. 9).

The influence of g_{q2}/g_{q1} and g_{r2}/g_{r1} ratios on the strain energy release rate is shown in Fig. 10. One can observe that the strain energy release rate decreases with increasing of g_{q2}/g_{q1} and g_{r2}/g_{r1} ratios (Fig. 10).

4. Conclusions

An approach for analyzing of delamination in non-linear viscoelastic multilayered beam structures subjected to bending in the plane of the layers is presented. The strain energy release rate derived here takes into account the non-linear viscoelastic behaviour, the change of the external loading on the beam with time and the material inhomogeneity (the layers exhibit continuous material inhomogeneity in longitudinal direction and as a result of this the material properties are functions of the longitudinal coordinate, x). In order to verify the solution, the strain energy release rate is found also by using the complementary strain energy in the beam structure. Solutions are used to perform parametric investigations. It is found that the strain energy release increases with time. The investigation reveals also that the strain energy release rate decreases with increasing of g_{E1}, g_{q1}, g_{r1}, g_{p1} and g_{f1}. The increase of g_{E2}/g_{E1}, g_{q2}/g_{q1} and g_{r2}/g_{r1} ratios leads also to decrease of the strain energy release rate. The analysis developed in this paper contributes to the understanding of the time-dependent delamination behaviour of non-linear viscoelastic multilayered inhomogeneous beams subjected to bending in the plane of the layers.

References

Ahmed, R.A., Fenjan, R.M. and Faleh, N.M. (2019), "Analyzing post-buckling behavior of continuously graded FG nanobeams with geometrical imperfections", *Geomech. Eng.*, **17**(2), 175-180. https://doi.org/10.12989/gae.2019.17.2.175.

Akbaş, Ş.D., Ersoy, H., Akgöz, B. and Civalek, Ö. (2021), "Dynamic analysis of a fiber-reinforced composite beam under a moving load by the Ritz method", *Math.*, **9**(9), 1048. https://doi.org/10.3390/math9091048.

Amara, K., Bouazza, M. and Fouad, B. (2016), "Postbuckling analysis of functionally graded beams using nonlinear model", *Periodica Polytechnica Mech. Eng.,* **60**(2), 121-128. https://doi.org/10.3311/PPme.8854.

Atmane, H.A., Bedia, E.A.A., Bouazza, M., Tounsi, A. and Fekrar, A. (2016). "On the thermal buckling of simply supported rectangular plates made of a sigmoid functionally graded Al/Al2O3 based material", *Mech. Solid.,* **51**, 177-187. https://doi.org/10.3103/S0025654416020059.

Becheri, T., Amara, K., Bouazza, M. and Benseddiq, N. (2016), "Buckling of symmetrically laminated plates using nth-order shear deformation theory with curvature effects", *Steel Compos. Struct.*, **21**(6), 1347-1368. https://doi.org/10.12989/scs.2016.21.6.1347.

Bouazza, M. and Zenkour, A.M. (2020), "Vibration of carbon nanotube-reinforced plates via refined *n*th-higher-order theory", *Arch. Appl. Mech.*, **90**, 1755-1769. https://doi.org/10.1007/s00419-020-01694-3.

Bouazza, M. and Benseddiq, N. (2015), "Analytical modeling for the thermoelastic buckling behavior of functionally graded rectangular plates using hyperbolic shear deformation theory under thermal loadings", *Multidisc. Model. Mater. Struct.*, **11**(4), 558-578. https://doi.org/10.1108/MMMS-02-2015-0008.

Bouazza, M. and Zenkour, A.M. (2020), "Hygro-thermo-mechanical buckling of laminated beam using hyperbolic refined shear deformation theory", *Compos. Struct.*, **252**, 112689. https://doi.org/10.1016/j.compstruct.2020.112689.

Bouazza, M., Amara, K., Zidour, M., Tounsi, A. and Adda-Bedia, E. (2014), "Hygrothermal effects on the postbuckling response of composite beam", *Am. J. Mater. Res.*, **1**(2), 35-43. http://www.aascit.org/journal/ajmr.

Bouazza, M., Antar, K., Amara, K. and Benyoucef, S. (2019), "Influence of temperature on the beams behavior strengthened by bonded composite plates", *Geomech. Eng.*, **18**(5), 555-566. https://doi.org/10.12989/gae.2019.18.5.555.

Bouazza, M., Becheri, T., Boucheta, A. and Benseddiq, N. (2019), "Bending behavior of laminated composite plates using the refined four-variable theory and the finite element method", *Earthq. Struct.*, **17**(3), 257-270. https://doi.org/10.12989/eas.2019.17.3.257.

Bouazza, M., Benseddiq, N. and Zenkour, A.M. (2019), "Thermal buckling analysis of laminated composite beams using hyperbolic refined shear deformation theory", *J. Therm. Stress.*, **42**(3), 332-340. https://doi.org/10.1080/01495739.2018.1461042.

Bouazza, M., Zenkour, A.M. and Benseddiq, N. (2018), "Effect of material composition on bending analysis of FG plates via a two-variable refined hyperbolic theory", *Arch. Mech.*, **70**(2), 1-23.

Butcher, R.J., Rousseau, C.E. and Tippur, H.V. (1999), "A functionally graded particulate composite: Measurements and failure analysis", *Acta Mater.*, **47**(2), 259-268. https://doi.org/10.1016/S1359-6454(98)00305-X.

Civalek, Ö., Akbas, S.D., Akgöz, B. and Dastjerdi, S. (2021), "Forced vibration analysis of composite beams reinforced by carbon nanotubes", *Nanomater.*, **11**, 571. https://doi.org/10.3390/nano 11030571.

Dastjerdi, S., Akgöz, B., Civalek, Ö., Malikan, M. and Eremeyev, V.A. (2020), "On the non-linear dynamics of torus-shaped and cylindrical shell structures", *Int. J. Eng. Sci.*, **156**, 103371. https://doi.org/10.1016/j.ijengsci.2020.103371.

Derbale, A., Bouazza, M. and Benseddiq, N. (2021), "Analysis of the mechanical and thermal buckling of laminated beams by new refined shear deformation theory", *Iran. J. Sci. Technol. Tran. Civil Eng.*, **45**, 89-98. https://doi.org/10.1007/s40996-020-00417-6.

Dolgov, N.A. (2005), "Determination of stresses in a two-layer coating", *Strength Mater.*, **37**(2), 422-431. https://doi.org/10.1007/s11223-005-0053-7.

Dolgov, N.A. (2016), "Analytical methods to determine the stress state in the substrate-coating system under mechanical loads", *Strength Mater.*, **48**(1), 658-667. https://doi.org/10.1007/s11223-016-9809-5.

Donaldson, S.L. (1988), "Mode III interlaminar fracture characterization of composite materials", *Compos. Sci. Technol.*, **32**, 225-249. https://doi.org/10.1016/0266-3538(88)90022-X.

Donaldson, S.L. and Mall, S. (1989), "Delamination growth in graphite/epoxy composite subjected to cyclic mode III loading", *J. Reinf. Plast. Compos.*, **8**, 91-103. https://doi.org/10.1177/073168448900800106.

El-Galy, I.M., Saleh, B.I. and Ahmed, M.H. (2019), "Functionally graded materials classifications and development trends from industrial point of view", *SN Appl. Sci.*, **1**, 1378. https://doi.org/10.1007/s42452-019-1413-4.

Ellali, M., Amara, K., Bouazza, M. and Bourada, F. (2018), "The buckling of piezoelectric plates on pasternak elastic foundation using higher-order shear deformation plate theories", *Smart Struct. Syst.*, **21**(1), 113-122. https://doi.org/10.12989/sss.2018.21.1.113.

Ellali, M., Bouazza, M. and Amara, K. (2022), "Thermal buckling of a sandwich beam attached with piezoelectric layers via the shear deformation theory", *Arch. Appl. Mech.,* **92**, 657-665. https://doi.org/10.1007/s00419-021-02094-x.

Ellali, M., Bouazza, M. and Zenkour, A.M. (2022), "Impact of micromechanical approaches on wave propagation of FG plates via indeterminate integral variables with a hyperbolic secant shear model", *Int. J. Comput. Meth.,* **19**(9), 2250019. https://doi.org/10.1142/S0219876222500190.

Faleh, N.M., Ahmed, R.A. and Fenjan, R.M. (2018), "On vibrations of porous FG nanoshells", *Int. J. Eng. Sci.*, **133**, 1-14. https://doi.org/10.1016/j.ijengsci.2018.08.007.

Fenjan, R.M., Ahmed, R.A., Alasadi, A.A. and Faleh, N.M. (2019), "Nonlocal strain gradient thermal

vibration analysis of doublecoupled metal foam plate system with uniform and non-uniform porosities", *Couple. Syst. Mech.*, **8**(3), 247-257. https://doi.org/10.12989/csm.2019.8.3.247.

Gasik, M.M. (2010), "Functionally graded materials: bulk processing techniques", *Int. J. Mater. Prod. Technol.*, **39**(1-2), 20-29. https://doi.org/10.1504/IJMPT.2010.034257.

Han, X., Xu, Y.G. and Lam, K.Y. (2001), "Material characterization of functionally graded material by means of elastic waves and a progressive-learning neural network", *Compos. Sci. Technol.*, **61**(10), 1401-1411. https://doi.org/10.1016/S0266-3538(01)00033-1**.**

Hedia, H.S., Aldousari, S.M., Abdellatif, A.K. and Fouda, N.A. (2014), "New design of cemented stem using functionally graded materials *(FGM)*", *Biomed. Mater. Eng.*, **24**(3), 1575-1588. https://doi.org/10.3233/BME-140962.

Hirai, T. and Chen, L. (1999), "Recent and prospective development of functionally graded materials in Japan", *Mater. Sci. Forum,* **308-311**(4), 509-514. https://doi.org/10.4028/www.scientific.net/MSF.308-311.509.

Lukash, P.A. (1978), *Fundamentals of Non-linear Structural Mechanics*, Stroiizdat.

Mahamood, R.M. and Akinlabi, E.T. (2017), *Functionally Graded Materials*, Springer.

Markworth, A.J., Ramesh, K.S. and Parks, Jr. W.P. (1995), "Review: modeling studies applied to functionally graded materials", *J. Mater. Sci.*, **30**(3), 2183-2193. https://doi.org/10.1007/BF01184560.

Miyamoto, Y., Kaysser, W.A., Rabin, B.H., Kawasaki, A. and Ford, R.G. (1999), *Functionally Graded Materials: Design, Processing and Applications*, Kluwer Academic Publishers, Dordrecht/London/Boston.

Nemat-Alla, M.M., Ata, M.H., Bayoumi, M.R. and Khair-Eldeen, W. (2011), "Powder metallurgical fabrication and microstructural investigations of Aluminum/Steel functionally graded material", *Mater. Sci. Appl.*, **2**(5), 1708-1718. https://doi.org/10.4236/msa.2011.212228.

Rizov, V. (2020), "Influence of the viscoelastic material behaviour on the delamination in multilayered beam", *Procedia Struct. Integr.*, **25**, 88-100. https://doi.org/10.1016/j.prostr.2020.04.013.

Rizov, V.I. (2020), "Analysis of two lengthwise cracks in a viscoelastic inhomogeneous beam structure", *Eng. Trans.*, **68**, 397-415. https://doi.org/10.24423/EngTrans.1214.20201125.

Rizov, V.I. (2021), "Delamination analysis of multilayered beams exhibiting creep under torsion", *Couple. Syst. Mech.*, **10**, 317-331. https://doi.org/10.12989/csm.2021.10.4.317.

Rizov, V.I. (2022), "Effects of periodic loading on longitudinal fracture in viscoelastic functionally graded beam structures", *J. Appl. Comput. Mech.*, **8**(1), 370-378. https://doi.org/10.22055/JACM.2021.37953.3141.

Rizov, V.I. and Altenbach, H. (2019), "Application of the classical beam theory for studying lengthwise fracture of functionally graded beams", *Technische Mechanik*, **39**(2), 229-240. https://doi.org/10.24352/UB.OVGU-2019-021.

Rizov, V.I. and Altenbach, H. (2022), "Multilayered frame structure subjected to non-linear creep: A delamination analysis", *Couple. Syst. Mech.*, **11**(3), 217-231. https://doi.org/10.12989/csm.2022.11.3.217 217.

Saiyathibrahim, A., Subramaniyan, R. and Dhanapl, P. (2016), "Centrefugally cast functionally graded materials-Review", *International Conference on Systems, Science, Control, Communications, Engineering and Technology*, 68-73.

Shrikantha Rao, S. and Gangadharan, K.V. (2014), "Functionally graded composite materials: an overview", *Procedia Mater. Sci.*, **5**(1), 1291-1299. https://doi.org/10.1016/j.mspro.2014.07.442.

Toudehdehghan, J., Lim, W., Foo1, K.E., Ma'arof, M.I.N. and Mathews, J. (2017), "A brief review of functionally graded materials", *MATEC Web of Conferences*, **131**, 03010. https://doi.org/10.1051/matecconf/201713103010UTP-UMP.

Wu, X.L., Jiang, P., Chen, L., Zhang, J.F., Yuan, F.P. and Zhu, Y.T. (2014), "Synergetic strengthening by gradient structure", *Mater. Res. Lett.*, **2**(1), 185-191. https://doi.org/10.1080/21663831.2014.935821.

AI

Nomenclature

A	crack area
a	crack length
b	beam width
C	integration constant
E	modulus of elasticity
f	material property describing the non-linear viscoelastic behaviour
G	strain energy release rate
g	parameter controlling the distribution of material properties along the beam length
h	beam height
l	beam length
M	bending moment
m	number of layers
p	material property describing the non-linear viscoelastic behaviour
q	material property describing the non-linear elastic behaviour
r	material property describing the non-linear elastic behaviour
t	time
U	strain energy
u	strain energy density
x	longitudinal axis
y	horizontal centric axis
z	vertical centric axis
ε	strain
ϕ	angle of rotation
η	coefficient of viscosity
κ	beam curvature
σ	stress